Brain Structure and Function (2019) 224:2297–2309
https://doi.org/10.1007/s00429-019-01905-w

ORIGINAL ARTICLE

The differential impact of acute microglia activation on the excitability of cholinergic neurons in the mouse medial septum

Orsolya Kékesi[1] · Huazheng Liang[1,3] · Gerald Münch[1] · John W. Morley[1] · Erika Gyengesi[1] · Yossi Buskila[1,2]

Received: 18 December 2018 / Accepted: 7 June 2019 / Published online: 13 June 2019

Abstract

The medial septal nucleus is one of the basal forebrain nuclei that projects cholinergic input to the hippocampus and cortex. Two of the hallmarks of Alzheimer's disease (AD) are a significant loss of cholinergic transmission and neuroinflammation, and it has been suggested that these two hallmarks are causally linked to the medial septum. Therefore, we have investigated the age-related susceptibility of medial septal cholinergic neurons to glial activation, mediated via peripheral administration of lipopolysaccharide (500 µg/kg) into *ChAT(BAC)-eGFP* mice at different ages (3–22 months). Our results show that during normal aging, cholinergic neurons experience a bi-phasic excitability profile, in which increased excitability at adulthood (ages ranging between 9 and 12 months) decreases in aged animals (> 18 months). Moreover, activation of glia had a differential impact on mice from different age groups, affecting K^+ conductances in young and adult animals, without affecting aged mice. These findings provide a potential explanation for the increased vulnerability of cholinergic neurons to neuroinflammation with aging as reported previously, thus providing a link to the impact of acute neuroinflammation in AD.

Keywords Neuroinflammation · Cholinergic neurons · Medial septum · Aging · Calcium homeostasis

Introduction

The cholinergic system in the brain is associated with multiple cognitive functions, including memory, selective attention, motivation and processing of emotion (Luchicchi et al. 2014). Most of the cholinergic projections to the cerebral cortex, the hippocampus, and the amygdala originate from the basal forebrain, a cholinergic complex comprising the medial septum nuclei, horizontal and vertical limbs of the diagonal band of Broca, and nucleus basalis of Meynert (Mesulam et al. 1983; Zaborszky et al. 2012).

Cholinergic neurons in the medial septum play an essential role in synaptic plasticity and memory formation in the hippocampus via the septohippocampal pathway, which also forms a feedback network (Zaborszky et al. 2015) found to be essential for spatial memory (Leung et al. 2003; Sava and Markus 2008; Martyn et al. 2012) and the maintenance of fear memories (Parfitt et al. 2012). However, previous studies showed that cholinergic neurons in the basal forebrain undergo moderate degenerative changes during aging, leading to a decrease in acetylcholine (ACh) release and memory deficits, reviewed by (Schliebs and Arendt 2006). Consistent with these studies, Markowska and colleagues showed that age-related memory deficits can be improved by either cholinergic stimulation (Markowska et al. 1995) or transplantation of ACh-secreting cells into the medial septum (Dickinson-Anson et al. 2003).

Degeneration of basal forebrain cholinergic cells has also been observed in several neurodegenerative diseases, including Parkinson's disease and Alzheimer's disease (AD) (Schliebs and Arendt 2006). Essentially, one hallmark of Alzheimer's disease is the degeneration of cholinergic neurons in the basal forebrain and the reduction of cholinergic innervation to cortical areas, which led to the development of the "cholinergic hypothesis" (Davies and Maloney 1976; Contestabile 2011; Craig et al. 2011). The mechanisms underlying the degeneration of cholinergic neurons during AD are still unknown, however previous reports suggest

✉ Yossi Buskila
Y.buskila@westernsydney.edu.au

1 School of Medicine, Western Sydney University, Campbelltown, NSW 2560, Australia

2 Biomedical Engineering and Neuroscience Research Group, The MARCS Institute, Western Sydney University, Penrith, NSW 2751, Australia

3 Shanghai Fourth People's Hospital, Tongji University, Shanghai, China

that acute and chronic inflammatory processes may play an important role, and thus should be investigated as a novel therapeutic target (Buskila et al. 2013a; Venigalla et al. 2016). Indeed, a previous study showed that the activity of cholinergic neurons from the basal forebrain of young rats (3 months old) declines within 2 weeks following induction of acute neuroinflammation via lipopolysaccharide (LPS) injections (Willard et al. 1999). The suggested mechanism underpinning the degeneration involved glutamate hyperexcitability via NMDA receptors that led to the cytotoxic release of calcium and nitric oxide. However, the particular vulnerability of cholinergic neurons to the neuroinflammatory processes in light of a normal age-related decline in cholinergic function is unknown. In order to assess the hypothesis that acute neuroinflammation affects the physiological properties of basal forebrain cholinergic neurons in an age-dependent manner, we have used electrophysiological and immunohistochemical tools to measure their excitability profile in different age groups.

Materials and methods

Animals

ChAT(BAC)-eGFP transgenic mice were obtained from Jax laboratories (strain 007902) and bred in house. All animals were healthy and handled with standard conditions of temperature, humidity, 12 h light/dark cycle, free access to food and water, and without any intended stress stimuli. All experiments were approved and performed in accordance with Western Sydney University committee for animal use and care guidelines (Animal Research Authority #A11199).

Induction of acute neuroinflammation

ChAT(BAC)-eGFP transgenic mice were divided into three age groups, corresponding to young (3–6 months, $n = 15$), adult (9–12 months, $n = 14$) and aged (18–22 months, $n = 6$) animals. Acute activation of microglia and astrocytes was induced via intraperitoneal injections of lipopolysaccharide (LPS; 500 µg/kg) on two consecutive days (Fig. 3a). The well-being of the animals was monitored throughout the procedure, and mice were killed 24 h after the last injection.

Slice preparation

Animals were deeply anesthetized by inhalation of isoflurane (5%), decapitated, and their brain was quickly removed and placed into artificial cerebrospinal fluid (aCSF) solution containing in mM: 125 NaCl, 2.5 KCl, 1 $MgCl_2$, 1.25 NaH_2PO_4, 2 $CaCl_2$, 25 $NaHCO_3$, 25 glucose and saturated with carbogen (95% O_2—5% CO_2 mixture; pH 7.4). Parasagittal brain slices (300 µm thick) which include the septohippocampal pathway [see Toth et al. (1997) and Chamberland et al. (2010) for detailed protocol] were cut with a vibrating microtome (Leica VT1200S) and transferred to the Braincubator™ (PaYo Scientific, Sydney; http://braincubator.com.au) as reported previously (Cameron et al. 2016). The Braincubator is an incubation system that closely monitors and controls pH, carbogen flow and temperature, as well as irradiating bacteria through a separate UV chamber (Breen and Buskila 2014; Buskila et al. 2014). Slices were initially incubated for 12 min at 35 °C, after which they were allowed to cool to 15–16 °C and kept in the Braincubator™ for at least 30 min before any measurement (Cameron et al. 2017). Images of the septohippocampal pathway were acquired using a Zeiss LSM-510 Meta confocal microscope (Carl Zeiss, Oberkochen, Germany) using a 40×-oil immersion objective in the inverted configuration, as previously reported (Breen and Buskila 2014; Zaman et al. 2016).

Electrophysiological recording and stimulation

The recording chamber was mounted on an Olympus BX-51 microscope equipped with IR/DIC optics. Following incubation in the Braincubator™, slices were mounted in the recording chamber for a minimum of 15 min, to allow them to warm up to room temperature (RT, ~ 22 °C), and were constantly perfused at a rate of 2–3 ml/min with carbogenated aCSF, as reported previously (Buskila and Amitai 2010).

Whole-cell intracellular recordings from *ChAT-eGFP* positive neurons in the medial septum were obtained with patch pipettes (5–7 MΩ) containing (in mM): 130 K-methylsulfate, 10 HEPES, 0.05 EGTA, 7 KCl, 0.5 Na_2GTP, 2 Na_2ATP, 2 MgATP, 7 phosphocreatine, and titrated with KOH to pH 7.2 (~ 285 mOsm). Voltages were recorded in current clamp mode using a multiclamp 700B dual patch-clamp amplifier (Molecular Devices), digitally sampled at 30–50 kHz, filtered at 10 kHz, and analyzed off-line using pClamp 10 software (Shlosberg et al. 2012; Buskila et al. 2013b). Cells were considered stable and suitable for analysis if the input resistance did not change more than 20% during the baseline recordings, before any treatment.

Suprathreshold sinusoidal stimulus protocol

In order to evaluate alterations in suprathreshold oscillation frequencies in the different conditions, we measured the sinusoidal–frequency curves as reported previously (Bellot-Saez et al. 2018). In short, 10-s stimulating protocols of sinusoidal current (chirp stimulation), in which there was a linear increase in the frequency from 0.1 to 100 Hz, were delivered at 30, 60, 125 and 250 pA, using the pClamp 10 software suite (Molecular Devices, Sunnyvale, CA, USA)

and injected into the neuronal soma through the recording electrode.

Enzyme-linked immunosorbent (ELISA) assay

Since we used the medial-septum sections for electrophysiological recordings, the level of TNFα was measured in the cerebellum. This way, while the measurements were not made from our area of interest, they were made from the same animals that we used for recording. Cerebellar hemispheres were homogenized with homogenizer followed by passing through a 21 and a 25 gauge syringe and finally sonicated for 5 min in lysis buffer containing (in mM): 1 EDTA, 1 EGTA; 1% Triton-X 100; 0.5% sodium deoxycholate with phosphatase inhibitors, such as 5 Na pyrophosphate, 25 NaF and 1 Na orthovanadate and protease inhibitor in 1:500 dilution. The homogenates were then centrifuged at 13,000 rpm for 20 min at 4 °C and supernatants were collected. Protein quantification was determined using the Bradford protein assay with gradient Bovine Serum Albumin solutions as a standard.

A commercial sandwich ELISA assay (Peprotech) was used to measure the level of TNFα in cerebellar homogenates. 96-well plates were covered and incubated with a capture antibody in a final concentration of 0.65 µg/ml (diluted in carbonate/bicarbonate buffer, pH 9.5) at 37 °C for 8 h followed by washing with PBS buffer (phosphate buffered saline, pH 7.2 with 0.05% Tween-20). The wells were then incubated with a blocking buffer (1% bovine serum albumin in PBS, pH 7.2) to eliminate nonspecific binding at RT for 1 h. After removal of the excess blocking buffer by washing, TNFα standards in serial dilution (from 0 to 10,000 pg/ml) in duplicates and the diluted protein samples in triplicates were added and incubated at 37 °C for 2 h. Following washing, homogenates were incubated with the detection antibody and avidin conjugated hydrogen peroxidase for 1.5 h at 37 °C followed by 30 min washing at RT. After washing the wells, the color development was induced by incubation with H_2O_2-containing (0.003%) 3,3,5,5-tetra methylbenzidine (TMB) solution containing dimethyl sulfoxide and H_2O_2 in Na_2HPO_4 and citric buffer, and the reaction was stopped by H_2SO_4 solution (0.03%). The absorbance was measured sequentially at wavelengths of 450 and 655 nm. The background (OD values at 655 nm) was subtracted before data analysis.

Immunohistochemistry

Immunohistochemical experiments were performed in order to confirm the activation of microglia. The brains were placed into PFA solution for 24 h followed by 30% sucrose solution for at least 24 h. 40-µm coronal sections which include the medial septum were cut with a Leica cryostat (Leica CM1950). Microglial activation was assessed via Iba-1 staining. Slices were incubated in PBS-based ethanol (50%)-H_2O_2 (1%) mixture for 20 min before they were transferred to the blocking solution (0.01% Triton-X and 5% goat serum in PBS) for 2 h. Rabbit anti-Iba-1 IgG (1:1000, Wako, #019–19741) was added to the blocking solution and slices were incubated on an orbital shaker for 12 h at RT. After washing the slices with PBS, secondary antibody (biotinylated goat-anti-rabbit IgG, 1:250, Life Technologies, #656140, or Alexa Fluor 594 conjugated goat-anti-rabbit IgG, 1:200, Jackson Immuno Research, #111-585-003) was applied and incubated for 2 h at RT. Incubation with avidin–biotin complex (1:250, Vector Laboratories, #PK-6100, in PBS and 0.1% Triton-X) was followed by a washing process. The staining was developed by incubation with 3′3-diaminobenzidine (DAB, 0.25 mg/ml) and induced by 0.0015% H_2O_2. Color development was monitored visually and stopped by placing the sections into PBS. The sections were mounted in anatomical order and after drying for 12 h, the sections were dehydrated in a serial dilution of EtOH from 50–70 to 95–100%, followed by xylene. The sections with the fluorescent secondary antibody were covered without the dehydration steps. Coverslips were placed with a mounting medium and imaged using a high magnification objective (x63, Zeiss Axio Imager M2). Cells were reconstructed with the Neurolucida 360 software (MBF Bioscience) and analyzed with its built-in analysis software (Neurolucida Explorer) to determine morphological features such as the size of the soma, as well as the number and length of the processes.

Data analysis

Data were analyzed with Prism 7 (GraphPad) and presented as mean ± SEM. Unless stated, one-way ANOVA or a *t* test was performed to determine the differences between age groups. A two-way ANOVA was employed to determine whether there were any significant interactions between the two treatments (saline and LPS) and age groups. A pair-wise multiple comparison procedure (Tukey test) was performed to test the differences between means. Statistical significance was defined as $p < 0.05$.

Results

The goal of this study was to assess the impact of acute activation of microglia on the physiological properties of cholinergic neurons in the septohippocampal pathway. As neuroinflammation was found to have a differential impact during aging (Isabelle Bardou et al. 2013), we also tested its impact at three different age groups corresponding to young

(4–6 months), adults (9–12 months) and aged (> 18 months) mice.

Basic membrane properties of cholinergic neurons in the medial septum

In order to study the impact of aging on cholinergic neurons in the medial septum, we have used single-cell electrophysiological recordings to monitor both passive and active membrane properties at different ages. Cholinergic neurons in the medial septum of *ChAT-eGFP* mice were identified by their green fluorescent signal, as shown in Fig. 1a, b, and showed active spiking properties following depolarizing stimuli (Fig. 1c). Our results indicate that during normal aging there is a significant depolarization of the resting membrane potential (RMP) of medial septum cholinergic neurons. While the average RMP in young animals was -59.7 ± 1 mV ($n = 23$), it significantly depolarized to -51.7 ± 1 mV in adult mice ($n = 15$) and -49.9 ± 3 mV in aged ($n = 5$) animals [F (5, 81) = 6.415, $p < 0.001$, one-way ANOVA with Tukey's post hoc test; Fig. 1d], indicating age-dependent alterations in the intrinsic excitability of cholinergic neurons, which did not affect the spike rheobase (F (2, 38) = 0.4803, $p = 0.6$, one-way ANOVA with Tukey's post hoc test; Fig. 1e) or input resistance [F (2, 35) = 2.421, $p = 0.1$, one-way ANOVA with Tukey's post hoc test].

However, recordings of the active membrane properties, such as spike amplitude and duration of the half-width spike amplitude (HWSA) showed a bi-phasic pattern, in which significant differences occurred only in adult animals (compared to the young age group) and returned to baseline levels (measurements recorded in young mice) in aged mice. While the spike amplitude was 102 ± 3 mV in young mice ($n = 19$), it significantly decreased to 91 ± 4 mV in adult animals ($n = 12$; $p < 0.05$) and increased back to 102 ± 5 mV in aged mice ($n = 8$, $p < 0.05$, one-way ANOVA with Fisher's

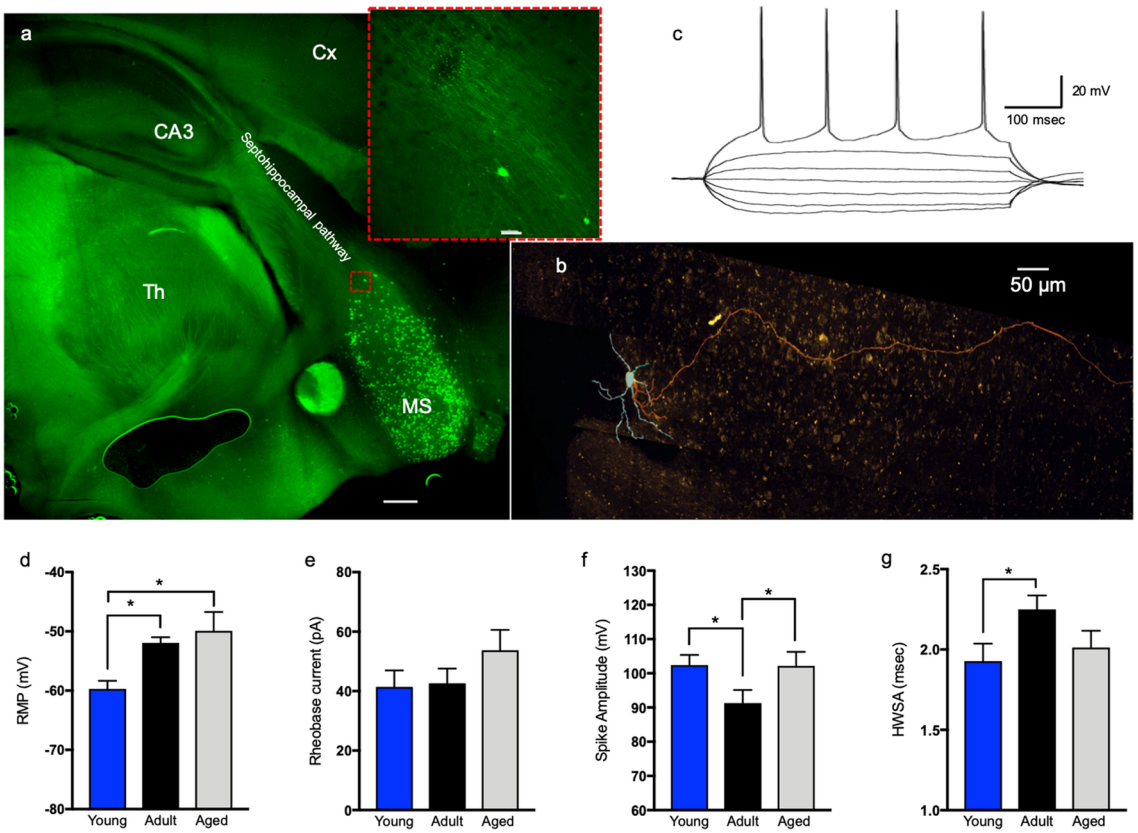

Fig. 1 Basic membrane properties of cholinergic neurons in the medial septum. **a** A representative confocal image of a septohippocampal brain slice from *ChAT-GFP* mouse depicting the spatial expression of cholinergic neurons (green) in the medial septum (MS) and their axons (insert, scale bar 50 µm) innervating CA3 region of the hippocampus. (Cx—cortex; Th—thalamus; scale bar 500 µm). **b** High-resolution image depicting the anatomical structure of a single $ChAT^{+}$ neuron in the medial septum filled with biocytin and reconstructed using Neurolucida 360 (scale bar 50 µm). **c** Sample traces of electrophysiological membrane properties of cholinergic neuron in response to both depolarizing and hyperpolarizing current injections. Bar plots depicting the average resting membrane potential (**d**), rheobase current (**e**), spike amplitude (**f**) and duration at half-width spike amplitude (**g**) in all age groups. Note the bi-phasic pattern of the spike amplitude and HWSA during aging, depicted as significant alterations in the adult group that return to baseline levels in aged animals. Data presented as mean ± SEM, *$p < 0.05$, one-way ANOVA

LSD test; Fig. 1f). In contrast, the HWSA was 1.9 ± 0.1 ms in young animals ($n = 14$) and increased to 2.3 ± 0.1 ms in adult mice ($n = 18$, $p < 0.05$) but did not increase significantly in aged animals (2.01 ± 0.1 ms; $n = 8$, Fig. 1g). As the spike width is highly dependent on K^+ conductance, these results indicate an intrinsic alteration in K^+ conductance.

To assess the ionic mechanisms underlying the alterations in K^+ conductances occurring with aging, we have measured the amplitude of membrane potentials that are associated with K^+ conductance, such as the 'sag' amplitude that portrays the H-current (I_h), as well as the fast and medium after-hyperpolarization potentials (AHP_f and AHP_m, respectively). AHP_f was measured following single spikes, while AHP_m was measured following bursts of action potentials (Fig. 2a), as previously described by Gu et al. (2005). Although the average AHP_f amplitude decreases with age, it was not significant between groups (Fig. 2b). However, the amplitude of the AHP_m potential displayed a bi-phasic pattern, in which a significant increase from 27.3 ± 4.9 mV in young mice to 53.33 ± 7.4 mV in adult animals ($p < 0.05$; one-way ANOVA with Fisher's LSD test), decreased to 31.8 ± 11.5 mV in aged mice (Fig. 2c). This bi-phasic pattern was similar to alterations seen in the sag amplitude, which significantly increased from an average amplitude of 11.95 ± 1.7 mV in young mice ($n = 16$) to 20.11 ± 3.7 mV in adult animals ($n = 12$) and then decreased to 11.1 ± 2.2 mV in aged mice [$n = 8$, F (5,

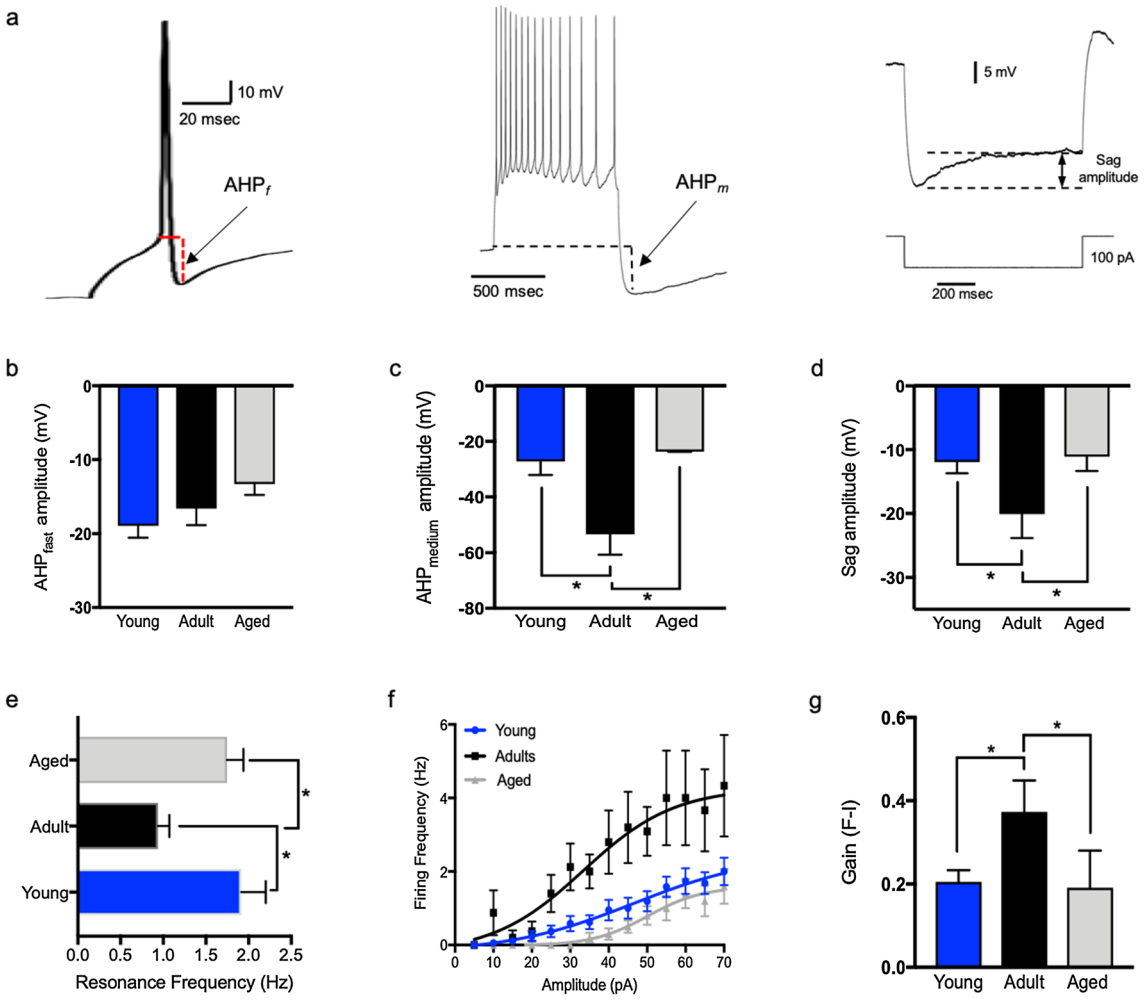

Fig. 2 Active membrane properties of cholinergic neurons express a bi-phasic excitability pattern during aging. **a** Sample traces of a single action potential (left), train of action potentials (middle) and hyperpolarization of the membrane potential (right) depicting the AHP_f, AHP_m and sag amplitude, respectively. Bar graphs depicting the average amplitude of the AHP_f (**b**), AHP_m (**c**) and sag amplitude (**d**) at different ages. Note the bi-phasic pattern of an increase of AHP_m and sag amplitude in the adult group, which return to baseline levels (recorded in the young age group) in aged animals. **e** Bar graph of the average resonance frequency at all age groups, which was significantly lower in the adult age group. **f** *F–I* curves describing the relationship between the current injected into cholinergic neurons and the firing frequency associated with the stimulus. The upward shift of the *F–I* curve in the adult group is indicative of increased excitability. **g** Bar plot depicting the average gain of the *F–I* curves, indicating significant alterations with the same bi-phasic pattern seen with other active membrane properties. Data presented as mean ± SEM, $^*p < 0.05$, one-way ANOVA

70) = 4.576, $p < 0.001$, one-way ANOVA with Fisher's LSD test; Fig. 2d]. Moreover, the resonance frequency which has been reported to be dependent on the interplay between the slowly activating K^+ current and a fast-persistent Na^+ current (Gutfreund et al. 1995), showed a similar bi-phasic phenomenon of significant decrease in adult animals (from 1.91 ± 0.2 Hz, $n = 16$, to 0.93 ± 0.1 Hz, $n = 15$) that increased in aged mice [1.74 ± 0.2 Hz, F (5, 57) = 5.088, $p < 0.01$, one-way ANOVA with Fisher's LSD test; Fig. 2e].

Neuronal spiking activity can be used to assess their overall excitability. In that regard, repetitive firing is a fundamental feature of spiking neurons, which determines their overall response to synaptic inputs during activation. We have therefore measured the firing frequency–current relationship (F–I curve) of cholinergic neurons following administration of step currents, as illustrated in Fig. 2f. Consistent with the bi-phasic pattern described above, the gain of the F–I curve significantly increased to 0.37 ± 0.07 in adult mice ($n = 9$) compared to young animals (0.2 ± 0.02; $n = 17$), and decreased in aged animals [0.19 ± 0.08, $n = 5$; F (5, 69) = 3.395, $p < 0.01$, one-way ANOVA with Fisher's LSD test; Fig. 2f, g]. These results are consistent with the alterations in the I_h and AHP_m currents, showing a bi-phasic characteristic, which underlies the involvement of K^+ conductance in the mechanisms determining the excitability of cholinergic neurons and their capacity for repetitive firing.

Microglial activation in ChAT-eGFP mice

Several methods can be used to induce and confirm acute neuroinflammation, among which, analysis of the morphological alterations of microglia (Vanguilder et al. 2011) and the expression level of Iba1 and TNFα are the most prominent. We induced microglia activation by intraperitoneal injections (IP) of lipopolysaccharide (LPS; 500 µg/kg) to *ChAT-eGFP* mice over two consecutive days (Fig. 3a). To validate the degree of glial activation in our animal model, we have analyzed both morphological alterations of microglial cells, as well as Iba1 and TNFα levels in the cerebellum, as shown in Fig. 3. This way, while the measurements were not made from our area of interest (medial septum), they were made from the very same animals that we used for recording. Sickness behavior appeared 2 h post-LPS injection and included reduced mobility, inactivity, ruffled fur, and decreased intake of water and food that led to a significant weight loss during the injection period, in all age groups. On average, the body weight 1 day post-LPS injection of young, adult and aged animals ($n = 15$, 14 and 6, respectively) decreased by 9.2 ± 0.6%, 8.2 ± 0.6% and 7.9 ± 0.7%, respectively, and further decreased by 3.9 ± 0.6%, 4 ± 0.6% and 4.6 ± 0.6%, respectively, following the second injection [F (1, 110) = 538, $p < 0.0001$, two-way ANOVA; Fig. 3b]. In contrast, the body weight of saline-injected animals from all age groups did not change during the injection period. The animals were killed 24 h following the second injection.

Our results show that following LPS injections, the level of TNFα increased significantly in all age groups, from (in pg/mg) 24.24 ± 2.94 to 41.26 ± 3.56 in young ($n = 5$), from 30 ± 2.78 to 51.59 ± 9.2 ($n = 9$) in adult and from 19.24 ± 1.25 to 57.88 ± 13.71 ($n = 4$) in aged animals [F (1, 36) = 10.82, $p = 0.0022$, two-way ANOVA with Tukey's post hoc test], confirming activation of microglia and the existence of acute neuroinflammation (Fig. 3c). Moreover, the soma size of microglial cells measured in the medial septum and hippocampus increased significantly following LPS treatment [F (1, 47) = 34.42, $p < 0.0001$, two-way ANOVA with Tukey's post hoc test; Fig. 4], from 45 ± 3 µm^2 ($n = 9$) to 80 ± 4 µm^2 ($n = 9$) in the medial septum and 35 ± 3 µm^2 ($n = 12$) to 61 ± 4 µm^2 ($n = 15$) in the hippocampus of young animals, 49 ± 3 µm^2 ($n = 9$) to 81 ± 9 µm^2 ($n = 9$) in the medial septum and 36 ± 3 µm^2 ($n = 9$) to 48 ± 3 µm^2 ($n = 15$) in the hippocampus

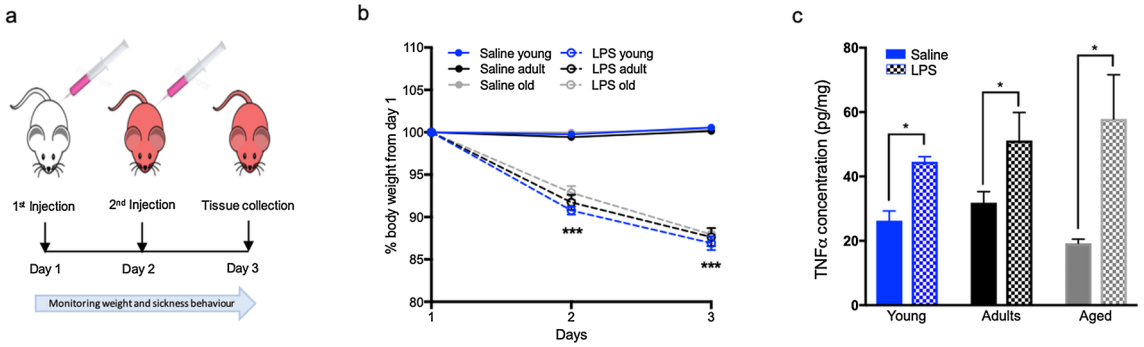

Fig. 3 Acute activation of glial cells. **a** Schematic diagram of the experimental plan for acute activation of glial cells. Each injection included LPS (500 µg/kg). Control animals were injected with saline. **b** Plot depicting the change in body weight as % from day 1 following LPS injections. **c** Bar graph depicting the increase in TNFα levels following LPS injections, indicative of induction of neuroinflammation. Data presented as mean ± SEM, *$p < 0.05$, ***$p < 0.001$, two-way ANOVA

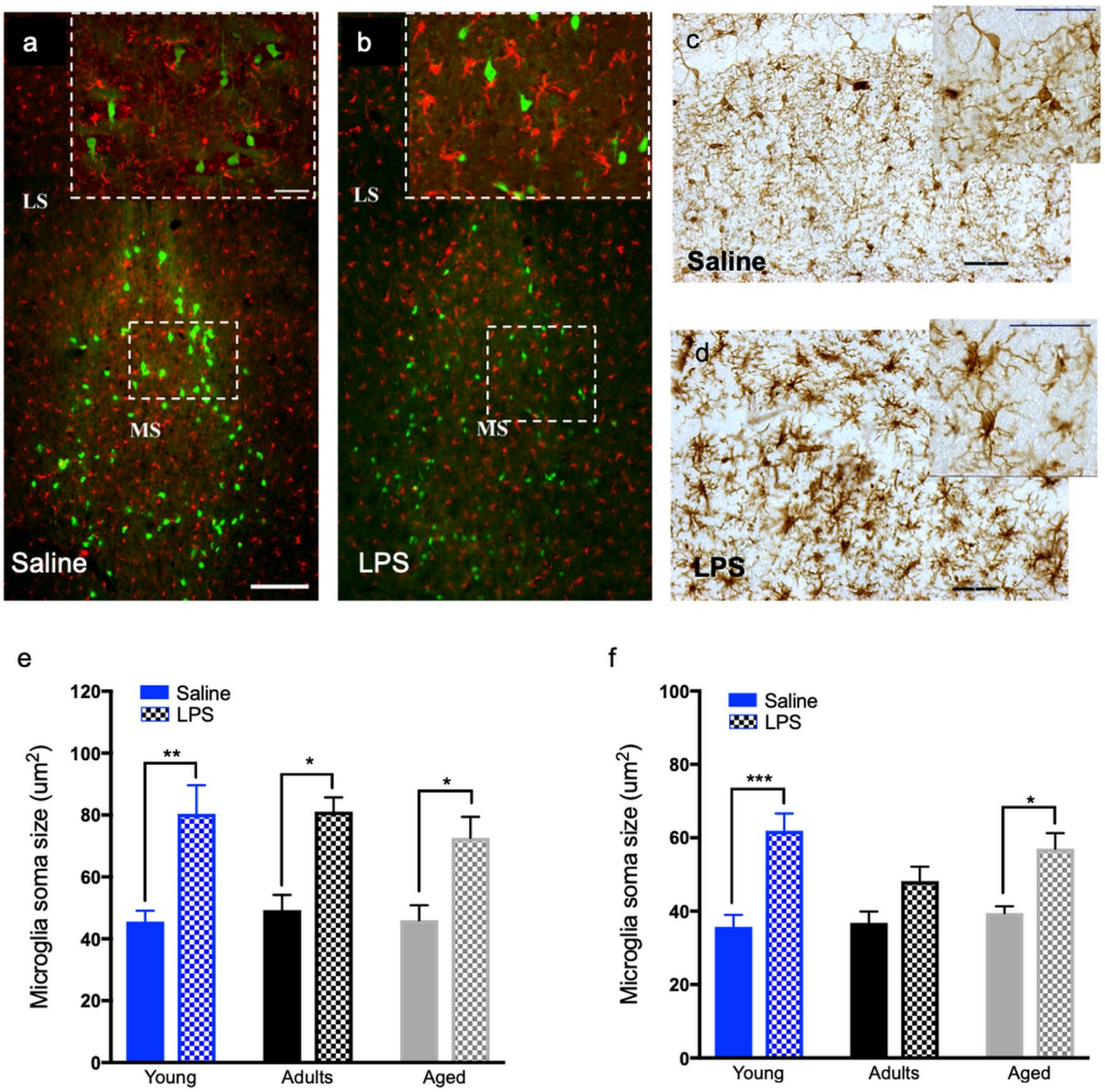

Fig. 4 Morphological alterations of microglia. **a**, **b** Confocal images (×20) of medial-septum brain slices with dual labeling for Iba-1 (red) and GFP-ChAT (green) from saline (**a**) and LPS (**b**) injected mice (scale bars 150 µm). Insets—high magnification (×40) images depicting morphological alterations in microglia (scale bar 50 µm). **c**, **d** Images of hippocampal brain slices with Iba-1 staining from saline (**c**) and LPS (**d**) injected mice depicting morphological alterations in microglia (scale bar 50 µm). Bar graphs depicting the changes in soma size of microglial cells in the medial septum (**e**) and hippocampus (**f**) following their activation by LPS. Data presented as mean ± SEM, $*p < 0.05$, $**p < 0.01$, $***p < 0.001$ two-way ANOVA

of adult animals and $46 \pm 8\ \mu m^2$ ($n = 9$) to $72 \pm 8\ \mu m^2$ ($n = 8$) in the medial septum and $39 \pm 2\ \mu m^2$ ($n = 9$) to $57 \pm 4\ \mu m^2$ ($n = 12$) in the hippocampus of aged animals, indicating that these microglia were in a 'primed' state, producing proinflammatory cytokines (Heneka et al. 2015; Torres-Platas et al. 2014).

Differential impact of glial activation on the excitability of medial septal cholinergic neurons

Recordings of the physiological properties of medial septum cholinergic neurons following LPS treatment indicate that glial activation has a differential impact on different age groups. While it did not affect the RMP, either between age groups nor within age groups (two-way ANOVA), activation of glial cells led to a significant increase in the input resistance only in mice from the adult age group [from 267 ± 28 MΩ, $n = 12$ to 394 ± 22 MΩ, $n = 21$, F (1, 79) = 7.833, $p < 0.01$, two-way ANOVA with Tukey's post hoc test; Fig. 5a]. This selective effect on the adult age group was accompanied by a significant decrease in the rheobase current (from 42 ± 7 to 25 ± 3 pA, $n = 20$, $p < 0.01$, Fig. 5b), as well as increase of the spike amplitude (from 91 ± 4 to 102.5 ± 2.3 mV, $p < 0.01$, Fig. 5c) and a decrease of the

HWSA (1.91 ± 0.08 ms, $p < 0.01$, two-way ANOVA with Tukey's post hoc test, Fig. 5d), suggesting an increase in the excitability profile of cholinergic neurons at this age, which is different to the bi-phasic excitability pattern seeing during normal aging (see Fig. 2).

Analysis of the afterhyperpolarization potentials showed that there were no significant alterations in the fast or the medium AHP potentials following LPS injections in all age groups tested (two-way ANOVA), however activation of glial cells led to a significant increase of the sag amplitude in young animals [from 11.9 ± 3.8 ($n = 16$) to 23.7 ± 3.4 mV ($n = 20$); F (1, 70) = 6.517, $p < 0.01$, two-way ANOVA with Tukey's post hoc test; Fig. 6a], without affecting the adult or aged groups. Moreover, activation of glia did not affect the neurons resonance frequency nor their responsiveness to electrical stimuli, as their repetitive firing abilities to increasing step currents were comparable to saline-injected mice (F–I curves, Fig. 6b, c), thus maintaining the age-dependent bi-phasic excitability profile.

In order to evaluate the relationship between membrane oscillation frequencies and spike threshold, we injected sinusoidal currents at different intensities (30–250 pA chirp current) at increasing frequencies (0.1–100 Hz; Fig. 6d). This protocol detects neuronal excitability at instantaneous sinusoidal frequencies and allows an evaluation of the relationship between neuronal excitability and oscillatory behavior (Bellot-Saez et al. 2018; Buskila et al. 2019), depicted by the frequency-spiking curve (SFC, Fig. 6e). Analysis of the sinusoidal–frequency curves of cholinergic neurons in the medial septum suggests that there were no significant differences between the various age groups or following LPS injections (two-way ANOVA, Fig. 6e, f). These results indicate that the maximal sinusoidal oscillatory frequency at which these neurons were still excitable was not affected by either age [F (1, 69) = 0.402, $p = 0.52$] or inflammation [F (2, 69) = 1.841, $p = 0.16$] and glial activation did not affect the overall responsiveness of cholinergic neurons to external inputs.

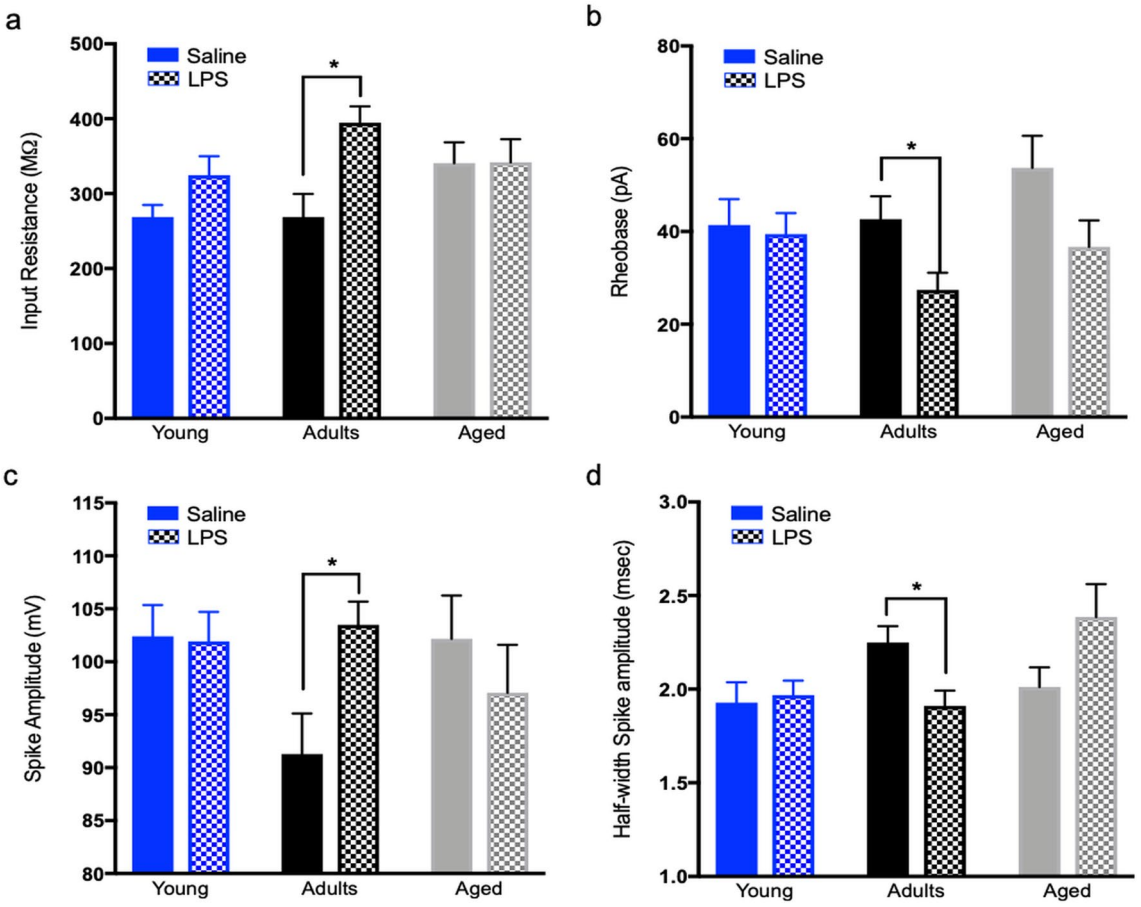

Fig. 5 Acute neuroinflammation has a differential impact on adult mice. Bar graph depicting the impact of LPS injections on the input resistance (**a**) and spike rheobase (**b**). Note the differential impact on the adult age group, without significant changes in the other age groups. Bar graphs depicting the impact of neuroinflammation on spike amplitude (**c**) and HWSA (**d**). Data presented as mean + SEM, $^*p < 0.05$

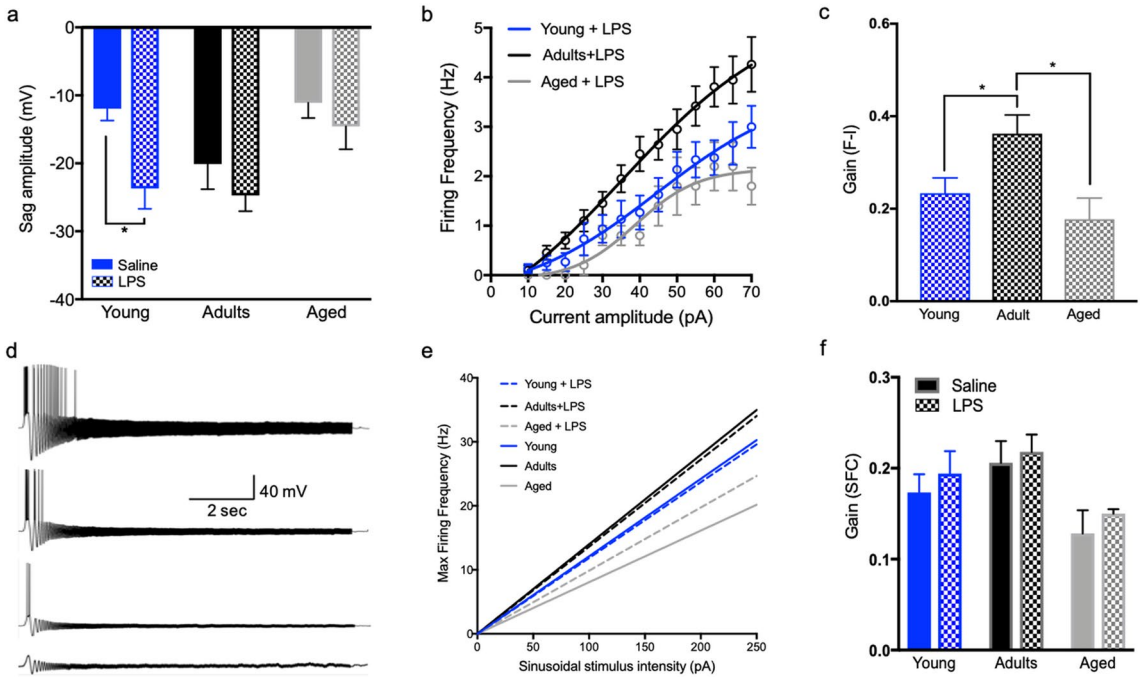

Fig. 6 Acute activation of glial cells did not affect the overall responsiveness of cholinergic neurons. **a** Bar graph depicting the impact of glial activation on the sag amplitude recorded in cholinergic neurons at different age groups (solid color-saline-injected mice, pattern-LPS injected mice). No significant differences were seen in either adult or aged animals. Plot of the *F–I* curves of cholinergic neurons recorded from LPS injected mice at different age groups (**b**) and bar graph (**c**) depicting the average gain of the *F–I* curves. Note the upward shift in the adult group, indicating a similar bi-phasic pattern seen during normal aging. **d** Sample voltage traces recorded following sinusoidal chirp stimulation (0.1–100 Hz) at different intensities (from bottom to top: 30 pA, 60 pA, 125 pA, 250 pA). **e** Sinusoidal–frequency spiking curves (SFCs; built using the chirp traces in **d**) depicting the relationship between the oscillation intensity and the maximal frequency at which the cell is still excitable. Note the upward shift in the maximal oscillation frequency in adult mice, indicative of increased responsiveness compared to the other age groups. **f** Bar graph depicting the average gain of the sinusoidal–frequency plots in all groups tested. $^*p < 0.05$; one-way ANOVA

Discussion

In order to assess the susceptibility of medial septum cholinergic neurons to acute neuroinflammation through aging, we have measured the impact of neuroinflammation (via activation of microglia) on their membrane properties within two days after LPS injections, while cholinergic neurons are still viable. Activation of microglial cells enhances the release of proinflammatory cytokines, including IL-1, IL-6, and TNFα as well as the upregulation of CD45, CD40 and major histocompatibility complex (MHC) class II molecules, (Yang et al. 2010; Ponomarev et al. 2014). In this study, we have used measurements of both TNFα and microglia morphology as an indirect indication of microglia activation, as previously reported by (Thameem Dheen et al. 2007; Kim et al. 2016). However, other neuroinflammatory markers such as MHC-II molecules and CD45 have been suggested to provide a more accurate approach to detect the extent of microglia activation.

Age-dependent bi-phasic alterations in the excitability profile of cholinergic neurons

Age-related alterations of cholinergic neurons in the medial septum have been previously studied in dissociated cell cultures, which have reduced synaptic connections, as well as a different excitability profile (Murchison et al. 2009). We therefore investigated the physiological properties of medial septal neurons in in vitro slice preparations, which better mimic their physiological environment (Buskila et al. 2014).

Our results indicate an age-dependent bi-phasic alteration in the physiological properties of medial septal cholinergic neurons during normal aging, depicted as increased excitability in adult animals that decreased in the aged group. To investigate the mechanisms underlying these alterations we have assessed their active properties. During normal aging, the adult age group shows a decrease in spike amplitude and an increase in the duration of the spike width (Fig. 1f, g), indicating an overall increase in voltage-dependent K^+ conductance that affects the repolarization phase of the action potential (Bean 2007). In cholinergic neurons, it has been proposed that the calcium-dependent large conductance

potassium channels (BK) and K_v4 channels are the ones that mostly contribute to the repolarization phase (Bean 2007). Hence, the increase in the spike half-width might be due to a functional decrease of Ca^{2+} channel activity as previously reported by (Faber and Sah 2003), or partial inactivation of the BK channels (Bean 2007). Indeed, previous reports indicated age-related bi-phasic alterations of Ca^{2+} buffering in cholinergic neurons that were also associated with impaired cognitive performance and altered synaptic transmission (Murchison et al. 2009; Griffith et al. 2014). However, significant changes in the functional activity or distribution of BK channels should also affect the fast spike afterhyperpolarization (AHP_f), which was not the case in our study (Fig. 2b), suggesting other processes may be superimposing and masking our results.

Spike afterhyperpolarization (AHP) consists of three temporally distinct currents termed fast AHP (AHP_f), medium AHP (AHP_m), and slow AHP (AHP_s) (Sah and Faber 2002). While the AHP_f is activated immediately after single spikes (< 10 ms) and is mediated by activation of BK channels, AHP_m lasts for 50–100 ms post-spike, is sensitive to apamin and mediated via small conductance (SK) and intermediate conductance (IK) potassium channels (Sah 1996). Calcium influx into neurons during spiking activity is mediated by high-voltage activated Ca^{2+} channels (e.g., L-type and N-type channels that activate BK, IK and SK channels), as well as low-voltage-activated calcium channels, that also activate SK channels (Scutt et al. 2015). However, calcium regulation is altered during aging (Oh et al. 2010), shifting towards release from internal stores (Foster 2007) rather than due to calcium influx through ionotropic receptors and voltage-gated calcium channels (VGCC), as shown in young animals. This shift affects calcium-dependent processes, including synaptic activity, AHP, and spiking behavior (Kumar and Foster 2004), which is consistent with our results.

Although our measurements of the AHP_f indicate a slight decrease through aging (Fig. 2b), the medium AHP and sag amplitude expressed an age-related bi-phasic pattern of increased amplitude in the adult mice (compared to young animals) that decreases in older animals from the aged group (Fig. 2c, d). The mechanism underlying the sag potential is the I_h current, mediated by hyperpolarization-activated cyclic nucleotide-gated cation (HCN) channels, which also affects the neurons resonance behavior and spiking output (Buskila et al. 2013b; Bellot-Saez et al. 2018). Indeed, our results indicate the same age-dependent bi-phasic pattern of both resonance and spiking frequency (Fig. 2e, f), suggesting that the overall excitability of cholinergic neurons in the adult age group is much higher than neurons recorded from both young and aged mice, and that the mechanism underpinning these alterations involves functional changes of HCN channels. Taken together, our results indicate that during normal aging, medial septum cholinergic neurons express multiple shifts in their physiological properties, which are mediated via modifications of K^+ conductances. However, the significance of the bi-phasic excitability profile to their normal function should be further investigated.

The differential impact of glial activation on K^+ conductance during aging

Neuroinflammation has been studied extensively in recent years, mainly due to its impact on brain pathology and association with CNS physiological activity (Di Filippo et al. 2008). Glial cells, mainly microglia and astrocytes, which are part of the immune system in the brain are also viewed as 'synaptic managers' (Bellot-Saez et al. 2017) and found to be involved in signal processing and modulation of network activity (Bellot-Saez et al. 2018). In that regard, it has been reported that major proinflammatory cytokines, such as IL-1β and TNFα can affect several forms of synaptic plasticity, such as LTP, in a dose-dependent manner (Goshen et al. 2007; Maggio and Vlachos 2018; Rizzo et al. 2018). While at low levels, IL-1β alters the conductance of NMDA receptors (Viviani et al. 2003), TNFα is able to increase the expression level of AMPA receptors in the hippocampus (Beattie et al. 2000), thus enhancing the synaptic efficacy and enlarge the size of the dendritic spines (Barnes et al. 2017). However, overexpression of neuroinflammatory molecules may result in neurodegeneration and impairment of synaptic plasticity (Katsuki et al. 1990; Vereker et al. 2000).

Animal models for acute neuroinflammation induced by LPS vary in several parameters, including the route of administration, range of doses (Fan et al. 2015; Tha et al. 2000), and injections intervals (Dias et al. 2005; Qin et al. 2007). Although several studies reported an upregulation in microglia numbers following acute neuroinflammation (Kitazawa 2005; Chen et al. 2012; Ifuku et al. 2012), we did not detect a significant difference in the number of microglial cells in any of the age groups [$F(1, 18) = 0.3632$, two-way ANOVA]. As the studies that reported on the upregulation of microglia applied high doses of LPS (at least 1000 mg/kg, Chen et al. 2012), or lower doses but for a longer time (Zivkovic et al. 2015), we assume that our method induced a low level of neuroinflammation that drove glia into a primed state (Lyman et al. 2014), as indicated by TNFα and Iba1 staining, with non-significant increase in the microglial proliferation.

Our results suggest that glial activation has a differential impact on the excitability of medial septal cholinergic neurons. On the one hand, LPS injections did not affect the input resistance or any of the active spiking properties (e.g., rheobase, spike amplitude, HWSA, and *F–I* curve; Fig. 5) of cholinergic neurons recorded from young animals. Yet, it led to a slight decrease in the resting

membrane potential and increase in the 'sag potential' in this age group (Fig. 6a). On the other hand, acute neuroinflammation led to hyperexcitability of cholinergic neurons recorded from the adult age group, displayed as a decrease in rheobase current (Fig. 5), which was accompanied by an increase of the input resistance and spike amplitude, along with a decrease of the spike width at half amplitude. Taken together, these results indicate a decrease of K^+ conductance, which is most likely due to dysregulation of Ca^{2+} homeostasis seen during both normal aging (Murchison et al. 2009) and neuroinflammation (Sama and Norris 2013). In aged animals, we did not see any significant differences, implying that a low level of acute neuroinflammation did not affect the elderly to the same extent as for younger animals.

The mechanism leading to enhanced susceptibility of cholinergic neurons following acute neuroinflammation is yet to be resolved, however, our data show clear alterations in the cellular excitability profile during normal aging, which is correlated with alterations in calcium buffering profile seen previously (Murchison et al. 2009; Griffith et al. 2014). As this bi-phasic pattern is seen across many physiological properties (e.g., spike amplitude, HWSA, AHP_m, I_h, input–output curves, and resonance frequency), we suggest it is critical for their viability and functional activity. Therefore, a possible reason for the enhanced vulnerability of cholinergic neurons following acute neuroinflammation is its impact on the excitability profile, specifically in the adult age group in which the bi-phasic pattern was abolished, probably through dysregulation of calcium homeostasis.

Previous studies on the impact of acute neuroinflammation on other brain areas, such as the hippocampus, showed that the input resistance and the intrinsic excitability were significantly increased in pyramidal neurons during acute neuroinflammation (Tzour et al. 2017), probably due to a decrease in K^+ conductance. However, the excitability profile of these neurons did not show the same pattern as cholinergic neurons, which might serve as a protective mechanism and therefore these cells were less vulnerable.

Acknowledgements This work was supported by seed funding grant (WSU) and Ainsworth Medical Research Innovation Fund to Y.B and E.G. O.K is supported by WSU postgraduate scholarship (UWSPRA).

Compliance with ethical standards

Conflict of interest The authors declare that they have no conflict of interest.

Ethical approval All procedures performed in this study involving animals were in accordance with the ethical standards of Western Sydney University (Animal Research Authority #A11199) at which the studies were conducted. This article does not contain any studies with human participants performed by any of the authors.

References

Bardou Isabelle, Brothers HM, Kaercher RM et al (2013) Differential effects of duration and age upon the consequences of neuroinflammation in the hippocampus. Neurobiol Aging 34:2293–2301. https://doi.org/10.1016/j.neurobiolaging.2013.03.034

Barnes SJ, Franzoni E, Jacobsen RI et al (2017) Deprivation-induced homeostatic spine scaling in vivo is localized to dendritic branches that have undergone recent spine loss. Neuron 96:871–882.e5. https://doi.org/10.1016/j.neuron.2017.09.052

Bean BP (2007) The action potential in mammalian central neurons. Nat Rev Neurosci 8:451–465. https://doi.org/10.1038/nrn2148

Beattie EC, Carroll RC, Yu X et al (2000) Regulation of AMPA receptor endocytosis by a signaling mechanism shared with LTD. Nat Neurosci 3:1291

Bellot-Saez A, Kékesi O, Morley JWJW, Buskila Y (2017) Astrocytic modulation of neuronal excitability through K^+ spatial buffering. Neurosci Biobehav Rev 77:87–97. https://doi.org/10.1016/j.neubiorev.2017.03.002

Bellot-Saez A, Cohen G, van Schaik A et al (2018) Astrocytic modulation of cortical oscillations. Sci Rep 8:11565. https://doi.org/10.1038/s41598-018-30003-w

Breen PP, Buskila Y (2014) Braincubator: an incubation system to extend brain slice lifespan for use in neurophysiology. In: Engineering in medicine and biology society (EMBC), 2014 36th annual international conference of the IEEE. IEEE, Chicago, pp 4864–4867

Buskila Y, Amitai Y (2010) Astrocytic iNOS-dependent enhancement of synaptic release in mouse neocortex. J Neurophysiol 103:1322–1328. https://doi.org/10.1152/jn.00676.2009

Buskila Y, Crowe SE, Ellis-Davies GCR (2013a) Synaptic deficits in layer 5 neurons precede overt structural decay in 5xFAD mice. Neuroscience 254:152–159

Buskila Y, Morley JW, Tapson J, van Schaik A (2013b) The adaptation of spike backpropagation delays in cortical neurons. Front Cell Neurosci 7:1–9. https://doi.org/10.3389/fncel.2013.00192

Buskila Y, Breen PP, Tapson J et al (2014) Extending the viability of acute brain slices. Sci Rep 4:4–10. https://doi.org/10.1038/srep05309

Buskila Y, Kékesi O, Bellot-Saez A et al (2019) Dynamic interplay between H-current and M-current controls motoneuron hyperexcitability in amyotrophic lateral sclerosis. Cell Death Dis 10:310. https://doi.org/10.1038/s41419-019-1538-9

Cameron M, Kékesi O, Morley JW et al (2016) Calcium imaging of AM dyes following prolonged incubation in acute neuronal tissue. PLoS One. https://doi.org/10.1371/journal.pone.0155468

Cameron MA, Kekesi O, Morley JW et al (2017) Prolonged incubation of acute neuronal tissue for electrophysiology and calcium-imaging. J Vis Exp 120:1–6. https://doi.org/10.3791/55396

Chamberland S, Salesse C, Topolnik D, Topolnik L (2010) Synapse-specific inhibitory control of hippocampal feedback inhibitory circuit. Front Cell Neurosci 4:1–14. https://doi.org/10.3389/fncel.2010.00130

Chen Z, Jalabi W, Shpargel KB et al (2012) Lipopolysaccharide-induced microglial activation and neuroprotection against experimental brain injury is independent of hematogenous TLR4. J Neurosci 32:11706–11715. https://doi.org/10.1523/JNEUROSCI.0730-12.2012

Contestabile A (2011) The history of the cholinergic hypothesis. Behav Brain Res 221:334–340. https://doi.org/10.1016/j.bbr.2009.12.044

Craig LA, Hong NS, McDonald RJ (2011) Revisiting the cholinergic hypothesis in the development of Alzheimer's disease. Neurosci Biobehav Rev 35:1397–1409. https://doi.org/10.1016/j.neubiorev.2011.03.001

Davies P, Maloney AJF (1976) Selective loss of central cholinergic neurons in Alzheimer's disease. Lancet 308:1403

Di Filippo M, Sarchielli P, Picconi B, Calabresi P (2008) Neuroinflammation and synaptic plasticity: theoretical basis for a novel, immune-centred, therapeutic approach to neurological disorders. Trends Pharmacol Sci 29:402–412. https://doi.org/10.1016/j.tips.2008.06.005

Dias MB, Almeida MC, Carnio EC et al (2005) Role of nitric oxide in tolerance to lipopolysaccharide in mice. J Appl Physiol 98:1322–1327. https://doi.org/10.1152/japplphysiol.01243.2004

Dickinson-Anson H, Winkler J, Fisher LJ et al (2003) Acetylcholine-secreting cells improve age-induced memory deficits. Mol Ther 8:51–61. https://doi.org/10.1016/S1525-0016(03)00145-X

Faber ESL, Sah P (2003) Ca^{2+}-activated K^+ (BK) channel inactivation contributes to spike broadening during repetitive firing in the rat lateral amygdala. J Physiol 552:483–497. https://doi.org/10.1113/jphysiol.2003.050120

Fan K, Li D, Zhang Y et al (2015) The induction of neuronal death by up-regulated microglial cathepsin H in LPS-induced neuroinflammation. J Neuroinflamm 12:1–12. https://doi.org/10.1186/s12974-015-0268-x

Foster TC (2007) Calcium homeostasis and modulation of synaptic plasticity in the aged brain. Aging Cell 6:319–325. https://doi.org/10.1111/j.1474-9726.2007.00283.x

Goshen I, Kreisel T, Ounallah-saad H et al (2007) A dual role for interleukin-1 in hippocampal-dependent memory processes. Psychoneuroendocrinology 32:1106–1115. https://doi.org/10.1016/j.psyneuen.2007.09.004

Griffith WH, DuBois DW, Fincher A et al (2014) Characterization of age-related changes in synaptic transmission onto F344 rat basal forebrain cholinergic neurons using a reduced synaptic preparation. J Neurophysiol 111:273–286. https://doi.org/10.1152/jn.00129.2013

Gu N, Vervaeke K, Hu H, Storm JF (2005) Kv7/KCNQ/M and HCN/h, but not KCa2/SK channels, contribute to the somatic medium after-hyperpolarization and excitability control in CA1 hippocampal pyramidal cells. J Physiol 566:689–715. https://doi.org/10.1113/jphysiol.2005.086835

Gutfreund Y, Yarom Y, Segev I (1995) Subthreshold oscillations and resonant frequency in guinea-pig cortical neurons: physiology and modelling. J Physiol 483(Pt 3):621–640

Heneka MT, Carson MJ, El Khoury J et al (2015) Neuroinflammation in Alzheimer's disease. Lancet Neurol 14:388–405. https://doi.org/10.1016/S1474-4422(15)70016-5

Ifuku M, Katafuchi T, Mawatari S et al (2012) Anti-inflammatory/anti-amyloidogenic effects of plasmalogens in lipopolysaccharide-induced neuroinflammation in adult mice. J Neuroinflammation 9:1–13. https://doi.org/10.1186/1742-2094-9-197

Katsuki H, Nakai S, Hirai Y et al (1990) Interleukin-1 beta inhibits long-term potentiation in the CA3 region of mouse hippocampal slices. Eur J Pharmacol 181:323–326. https://doi.org/10.1016/0014-2999(90)90099-R

Kim H-Y, Lee J-W, Chen H et al (2016) *N*-Docosahexaenoylethanolamine ameliorates LPS-induced neuroinflammation via cAMP/PKA-dependent signaling. J Neuroinflamm 13:1–15. https://doi.org/10.1186/s12974-016-0751-z

Kitazawa M (2005) Lipopolysaccharide-induced inflammation exacerbates tau pathology by a cyclin-dependent kinase 5-mediated pathway in a transgenic model of Alzheimer's disease. J Neurosci 25:8843–8853. https://doi.org/10.1523/JNEUROSCI.2868-05.2005

Kumar A, Foster TC (2004) Enhanced long-term potentiation during aging is masked by processes involving intracellular calcium stores. J Neurophysiol 91:2437–2444. https://doi.org/10.1152/jn.01148.2003

Leung LS, Shen B, Rajakumar N, Ma J (2003) Cholinergic activity enhances hippocampal long-term potentiation in CA1 during walking in rats. J Neurosci 23:9297–9304 **(pii: 23/28/9297)**

Luchicchi A, Bloem B, Viaña JNM et al (2014) Illuminating the role of cholinergic signaling in circuits of attention and emotionally salient behaviors. Front Synaptic Neurosci 6:1–10. https://doi.org/10.3389/fnsyn.2014.00024

Lyman M, Lloyd DG, Ji X et al (2014) Neuroinflammation: the role and consequences. Neurosci Res 79:1–12. https://doi.org/10.1016/j.neures.2013.10.004

Maggio N, Vlachos A (2018) Tumor necrosis factor (TNF) modulates synaptic plasticity in a concentration-dependent manner through intracellular calcium stores. J Mol Med (Berl). https://doi.org/10.1007/s00109-018-1674-1

Markowska AL, Olton DS, Givens B (1995) Cholinergic manipulations in the medial septal area: age-related effects on working memory and hippocampal electrophysiology. J Neurosci 15:2063–2073

Martyn AC, De Jaeger X, Magalhaes AC et al (2012) Elimination of the vesicular acetylcholine transporter in the forebrain causes hyperactivity and deficits in spatial memory and long-term potentiation. Proc Natl Acad Sci 109:17651–17656. https://doi.org/10.1073/pnas.1215381109

Mesulam M-M, Mufson EJ, Levey AI, Wainer BH (1983) Cholinergic innervation of cortex by the basal forebrain: cytochemistry and cortical connections of the septal area, diagonal band nuclei, nucleus basalis (Substantia innominata), and hypothalamus in the rhesus monkey. J Comp Neurol 214:170–197. https://doi.org/10.1002/cne.902140206

Murchison D, McDermott AN, Lasarge CL et al (2009) Enhanced calcium buffering in F344 rat cholinergic basal forebrain neurons is associated with age-related cognitive impairment. J Neurophysiol 102:2194–2207. https://doi.org/10.1152/jn.00301.2009

Oh MM, Oliveira FA, Disterhoft JF (2010) Learning and aging related changes in intrinsic neuronal excitability. Front Aging Neurosci 2:1–10. https://doi.org/10.3389/neuro.24.002.2010

Parfitt GM, Campos RC, Barbosa ÂK et al (2012) Participation of hippocampal cholinergic system in memory persistence for inhibitory avoidance in rats. Neurobiol Learn Mem 97:183–188. https://doi.org/10.1016/j.nlm.2011.12.001

Ponomarev ED, Shriver LP, Dittel BN (2014) CD40 expression by microglial cells is required for their completion of a two-step activation process during central nervous system autoimmune inflammation. J Immunol 176:1402–1410. https://doi.org/10.4049/jimmunol.176.3.1402

Qin L, Wu X, Block ML et al (2007) Systemic LPS causes chronic neuroinflammation and progressive neurodegeneration. Glia 55:453–462. https://doi.org/10.1002/glia.20467.Systemic

Rizzo FR, Musella A, De Vito F et al (2018) Tumor necrosis factor and interleukin-1β modulate synaptic plasticity during neuroinflammation. Neural Plast 2018:8430123. https://doi.org/10.1155/2018/8430123

Sah P (1996) Ca^{2+}-activated K^+ currents in neurones: types, physiological roles and modulation. Trends Neurosci 19(4):150–154

Sah P, Faber ESL (2002) Channels underlying neuronal calcium-activated potassium currents. Prog Neurobiol 66(5):345–353

Sama DM, Norris CM (2013) Calcium dysregulation and neuroinflammation: discrete and integrated mechanisms for age-related synaptic dysfunction Diana. Ageing Res Rev 12:1–27. https://doi.org/10.1016/j.neuroimage.2013.08.045.The

Sava S, Markus EJ (2008) Activation of the medial septum reverses age-related hippocampal encoding deficits: a place field analysis. J Neurosci 28:1841–1853. https://doi.org/10.1523/JNEUROSCI.4629-07.2008

Schliebs R, Arendt T (2006) The significance of the cholinergic system in the brain during aging and in Alzheimer's disease. J

Neural Transm 113:1625–1644. https://doi.org/10.1007/s00702-006-0579-2

Scutt G, Allen M, Kemenes G, Yeoman M (2015) A switch in the mode of the sodium/calcium exchanger underlies an age-related increase in the slow afterhyperpolarization. Neurobiol Aging 36:2838–2849. https://doi.org/10.1016/j.neurobiolaging.2015.06.012

Shlosberg D, Buskila Y, Abu-Ghanem Y, Amitai Y (2012) Spatiotemporal alterations of cortical network activity by selective loss of NOS-expressing interneurons. Front Neural Circ 6:1–11. https://doi.org/10.3389/fncir.2012.00003

Tha KK, Okuma Y, Miyazaki H et al (2000) Changes in expressions of proinflammatory cytokines IL-1beta, TNF-alpha and IL-6 in the brain of senescence accelerated mouse (SAM) P8. Brain Res 885:25–31. https://doi.org/10.1016/S0006-8993(00)02883-3

Thameem Dheen S, Kaur C, Ling E-A (2007) Microglial activation and its implications in the brain diseases. Curr Med Chem 14:1189–1197. https://doi.org/10.2174/092986707780597961

Torres-Platas SG, Comeau S, Rachalski A et al (2014) Morphometric characterization of microglial phenotypes in human cerebral cortex. J Neuroinflamm 11:12. https://doi.org/10.1186/1742-2094-11-12

Toth K, Freund TF, Miles R (1997) Disinhibition of rat hippocampal pyramidal cells by GABAergic afferents from the septum. J Physiol 500:463–474

Tzour A, Leibovich H, Barkai O et al (2017) KV 7/M channels as targets for lipopolysaccharide-induced inflammatory neuronal hyperexcitability. J Physiol 595:713–738. https://doi.org/10.1113/JP272547

Vanguilder HD, Bixler GV, Brucklacher RM et al (2011) Concurrent hippocampal induction of MHC II pathway components and glial activation with advanced aging is not correlated with cognitive impairment. J Neuroinflamm 8:138. https://doi.org/10.1186/1742-2094-8-138

Venigalla M, Sonego S, Gyengesi E et al (2016) Novel promising therapeutics against chronic neuroinflammation and neurodegeneration in Alzheimer's disease. Neurochem Int 95:63–74. https://doi.org/10.1016/j.neuint.2015.10.011

Vereker E, O'Donnell E, Lynch MA (2000) The inhibitory effect of interleukin-1 beta on long-term potentiation is coupled with increased activity of stress-activated protein kinases. J Neurosci 20:6811–6819 **(pii: 20/18/6811)**

Viviani B, Bartesaghi S, Gardoni F et al (2003) Interleukin-1beta enhances NMDA receptor-mediated intracellular calcium increase through activation of the Src family of kinases. J Neurosci 23:8692–8700 **(pii: 23/25/8692)**

Willard B, Hauss-Wegrzyniak B, Wenk GL (1999) Pathological and biochemical consequences of acute and chronic neuroinflammation within the basal forebrain cholinergic system of rats. Neuroscience 88:193–200. https://doi.org/10.1016/S0306-4522(98)00216-4

Yang I, Han SJ, Kaur G et al (2010) The role of microglia in central nervous system immunity and glioma immunology. J Clin Neurosci 17:6–10. https://doi.org/10.1016/j.jocn.2009.05.006

Zaborszky L, Pol A Van Den, Gyengesi E (2012) The basal forebrain cholinergic projection system in mice. In: Watson C, Paxinos G, Puelles L (eds) The mouse nervous system. Academic Press, New York, pp 684–718

Zaborszky L, Csordas A, Mosca K et al (2015) Neurons in the basal forebrain project to the cortex in a complex topographic organization that reflects corticocortical connectivity patterns: an experimental study based on retrograde tracing and 3D reconstruction. Cereb Cortex 25:118–137. https://doi.org/10.1093/cercor/bht210

Zaman MS, Johnson AJ, Bobek G et al (2016) Protein kinase CK2 regulates metal toxicity in neuronal cells. Metallomics 8:82–90. https://doi.org/10.1039/C5MT00260E

Zivkovic AR, Sedlaczek O, von Haken R et al (2015) Muscarinic M1 receptors modulate endotoxemia-induced loss of synaptic plasticity. Acta Neuropathol Commun 3:67. https://doi.org/10.1186/s40478-015-0245-8